

Electronic Supplementary Information

Boosting reverse intersystem crossing by increasing donors in triarylboron/phenoxazine hybrids: TADF emitters for high-performance solution-processed OLEDs

*Yuan Liu,^a Guohua Xie,^a Kailong Wu,^a Zhenghui Luo,^a Tao Zhou,^a Xuan Zeng,^a Jie Yu,^a Shaolong Gong^a and Chuluo Yang^{*a,b}*

^a Hubei Collaborative Innovation Center for Advanced Organic Chemical Materials, Hubei Key Lab on Organic and Polymeric Optoelectronic Materials, Department of Chemistry, Wuhan University, Wuhan, 430072, People's Republic of China.

^b New Materials Technology Institute, Co-Innovation Center for Micro/Nano Optoelectronic Materials and Devices, Chongqing University of Arts and Sciences, Chongqing, 402160, People's Republic of China.

Corresponding Author

**E-mail: clyang@whu.edu.cn (Chuluo Yang)*

General information

All the reagents and solvents used for the synthesis or measurements were commercially available, and used as received unless otherwise stated.

The ^1H NMR and ^{13}C NMR spectra were recorded on a MERCURY-VX300 spectrometer with CDCl_3 as the solvent and tetramethylsilane as an internal reference. EI mass spectra were determined by a ZAB 3F-HF mass spectrophotometer. Elemental analyses were performed on a Vario EL-III microanalyzer. Cyclic voltammetry (CV) was carried out in nitrogen-purged dichloromethane (oxidation scan) at room temperature with a CHI voltammetric analyzer. $n\text{-Bu}_4\text{PF}_6$ (0.1 M) was used as the supporting electrolyte. The conventional three-electrode configuration consists of a platinum working electrode, a platinum wire auxiliary electrode, and an Ag wire pseudo-reference electrode with ferrocene (Fc/Fc^+) as the internal standard. The onset potential was determined from the intersection of two tangents drawn at the rising and background current of the cyclic voltammogram. The HOMO energy levels (eV) of the compounds were calculated according to the formula: $-[4.8+(E_{\text{onset}}-E_{1/2(\text{Fc}/\text{Fc}^+)})]\text{eV}$. Differential scanning calorimetry (DSC) was performed on a NETZSCH DSC 200 PC unit at a heating rate of $20\text{ }^\circ\text{C min}^{-1}$ from 20 to $450\text{ }^\circ\text{C}$ under argon. The glass transition temperature (T_g) was determined from the second heating scan at a heating rate of $10\text{ }^\circ\text{C min}^{-1}$. UV-vis absorption spectra were recorded on a Shimadzu UV-2700 recording spectrophotometer. Photoluminescence (PL) spectra were recorded on a Hitachi F-4600 fluorescence spectrophotometer. The PL lifetimes was measured by a single photon counting spectrometer from Edinburgh Instruments (FLS920) with a Picosecond Pulsed UV-LASTER (LASTER377) as the excitation source. Absolute PLQYs were obtained using a Quantaurus-QY measurement system (C11347-11, Hamamatsu Photonics) and all the samples were excited at 330 nm .

Device fabrication and characterization

The ITO substrates were degreased in acetone and ethanol consecutively in an ultrasonic bath before UV-ozone treatment for 10 minutes. A layer of 30 nm thick PEDOT:PSS was spin-coated onto the ITO substrate and then baked at $120\text{ }^\circ\text{C}$ for 10 minutes. Another baking at $100\text{ }^\circ\text{C}$ for 10 minutes was conducted after spin-coating of the emitting layer. A layer of TmPyPB, served as the electron transporting layer, was thermally deposited onto the emitting layer. After the evaporation of the composite Liq/Al cathode, the devices were encapsulated with UV-curable resin. The current-voltage-luminance characteristics and the EL spectra were measured simultaneously by a customized software controlling a PR735 spectrometer and a Keithley 2400 source measurement unit. The power efficiency and the external quantum efficiency were calculated by assuming a Lambertian emission profile.

Computation details

Quantum chemical calculations were performed with the hybrid DFT functional Becke and Hartree-Fock exchange and Lee Yang and Parr correlation (B3LYP) using the Gaussian 09 program packages.

The ground state molecular structures were optimized at the B3LYP/6-31g(d) level of theory. The time-dependent DFT (TD-DFT) calculations were performed using LC- ω *PBE theory reported by Brédas and coworkers.¹

Synthesis of materials

Tris(4-bromo-2,3,5,6-tetramethylphenyl)borane was prepared according to the literature.²

To a mixture of tris(4-bromo-2,3,5,6-tetramethylphenyl)borane (1.05 g, 1.55 mmol), 10*H*-phenoxazine (1.42 g, 7.75 mmol), palladium acetate (54 mg, 0.23 mmol), tri-*tert*-butylphosphine tetrafluoroborate (210 mg, 0.69 mmol) and sodium *tert*-butoxide (540 mg, 5.58 mmol) were added redistilled toluene (20 mL), and the solution was refluxed for 48h under argon. The resulting mixture was poured into water and extracted with chloroform. The combined organic layer was washed with water, and dried over Na₂SO₄. After removed the solvent under reduced pressure, the residue was purified with a silicone gel column using *n*-hexane/chloroform (5:1, v/v) as the eluent to obtain the final products and further recrystallization from a mixed solution of chloroform/*n*-hexane with yields of 35%, 15% and 10% for TB-3PXZ (yellow powder), TB-2PXZ (light-yellow powder) and TB-1PXZ (off-white powder), respectively.

10-(4-(bis(2,3,5,6-tetramethylphenyl)boranyl)-2,3,5,6-tetramethylphenyl)-10*H*-phenoxazine (**TB-1PXZ**): ¹H NMR(CDCl₃, 300 MHz) δ (ppm): 6.96 (s, 2H; ArH), 6.64-6.59 (m, 6H; ArH), 5.68 (s, 2H; ArH), 2.20 (s, 6H; CH₃), 2.16 (s, 6H; CH₃), 2.07 (s, 6H; CH₃), 2.02 (s, 6H; CH₃), 2.00 (s, 6H; CH₃), 1.94 (s, 6H; CH₃). ¹³C NMR (CDCl₃, 75 MHz) δ (ppm): 150.2, 148.9, 143.8, 138.7, 138.0, 136.0, 135.3, 133.6, 132.6, 123.6, 121.0, 115.3, 114.3, 112.0, 20.5, 19.5, 14.7, 14.3. MS (EI, m/z): 680.4 [M]⁺. Anal. calcd for C₄₂H₄₆BNO: C 85.26, H 7.84, N 2.37; found: C 85.53, H 7.86, N 2.37.

10,10'-(((2,3,5,6-tetramethylphenyl)boranediy))bis(2,3,5,6-tetramethyl-4,1-phenylene))bis(10*H*-phenoxazine) (**TB-2PXZ**): ¹H NMR(CDCl₃, 300 MHz) δ (ppm): 7.00 (s, 1H; ArH), 6.67-6.60 (m, 12H; ArH), 5.68 (s, 4H; ArH), 2.22 (s, 6H; CH₃), 2.13-2.10 (m, 18H; CH₃), 2.06 (s, 6H; CH₃), 2.03 (s, 6H; CH₃). ¹³C NMR (CDCl₃, 75 MHz) δ (ppm): 150.0, 148.7, 143.9, 138.4, 138.0, 136.0, 135.3, 134.0, 133.6, 132.6, 123.6, 121.0, 115.3, 112.0, 20.3, 19.3, 14.5, 14.4. MS (EI, m/z): 772.8 [M]⁺. Anal. calcd for C₅₄H₅₃BN₂O₂: C 83.92, H 6.91, N 3.62; found: C 84.29, H 6.93, N 3.63.

Tris(2,3,5,6-tetramethyl-4-(10*H*-phenoxazin-10-yl)phenyl)borane (**TB-3PXZ**): ¹H NMR(CDCl₃, 300 MHz) δ (ppm): 6.66-6.59 (m, 18H; ArH), 5.69 (s, 6H; ArH), 2.15 (s, 36H; CH₃). ¹³C NMR (CDCl₃, 75 MHz) δ (ppm): 149.7, 143.8, 138.1, 134.5, 132.2, 123.5, 120.9, 115.2, 111.9, 20.4, 14.5. MS (EI, m/z): 954.1 [M]⁺. Anal. calcd for C₆₆H₆₀BN₃O₃: C 83.09, H 6.34, N 4.40; found: C 83.44, H 6.36, N 4.41.

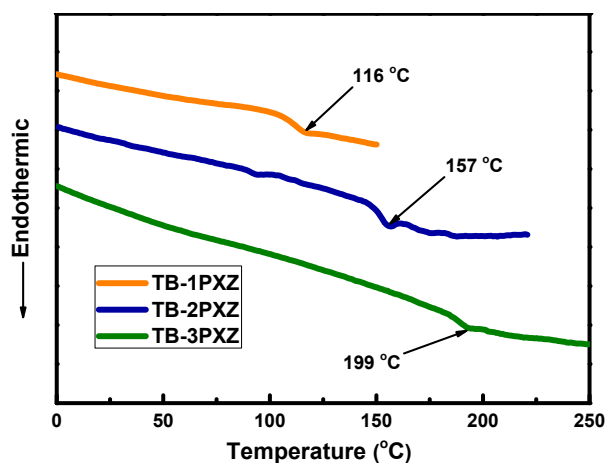


Fig. S1. DSC curves of TB-1PXZ, TB-2PXZ and TB-3PXZ.

Table S1. Values from DFT calculation.

Compound	α^a (°)	HOMO (eV)	LUMO (eV)	S_1 (eV)	T_1 (eV)	ΔE_{ST} (eV)
TP-1PXZ	87.5	-4.54	-1.58	3.28	2.79	0.49
TP-2PXZ	87.3	-4.61	-1.78	2.99	2.78	0.21
TP-3PXZ	87.4	-4.68	-1.98	2.74	2.73	0.01

^a)Dihedral angles of phenyl plane and adjacent phenoxazine plane.

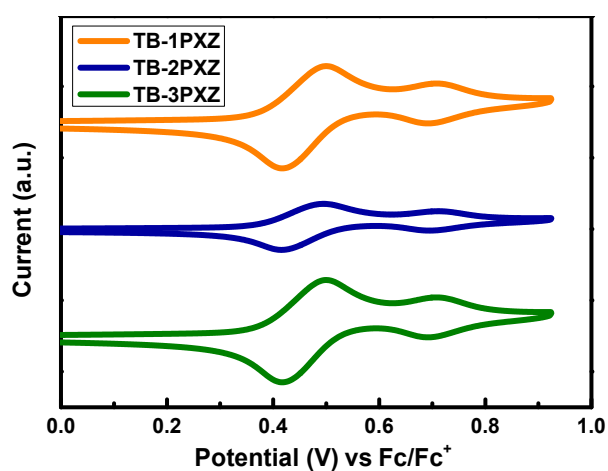


Fig. S2. Oxidation behaviors of TB-1PXZ, TB-2PXZ and TB-3PXZ.

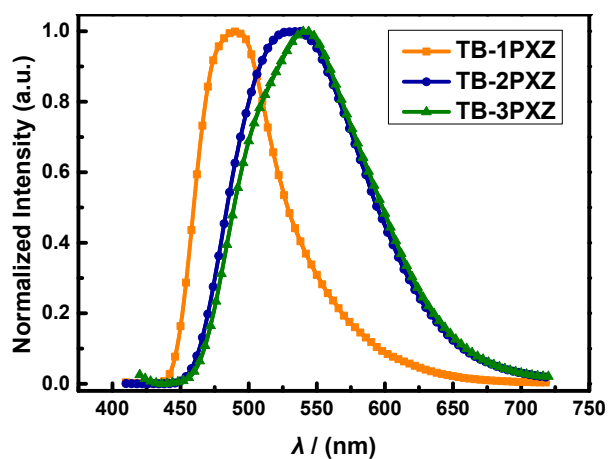


Fig. S3. Phosphorescence spectra of TB-1PXZ, TB-2PXZ and TB-3PXZ in film.

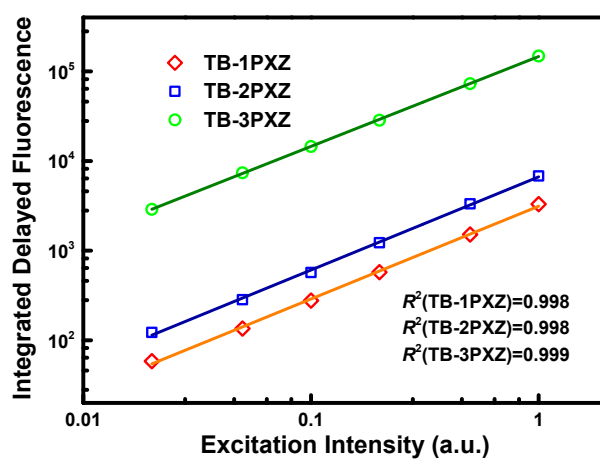


Fig. S4. The linear dependence of the integrated delayed fluorescence on laser excitation intensity.

$$EQE = \gamma n_{\text{out}} \left[0.25\Phi_{\text{PL}} + 0.75 \frac{\Phi_{\text{d}}}{1 - (\Phi_{\text{PL}} - \Phi_{\text{d}})} \right] \quad \text{Equation S1}$$

Reference

1. H. Sun, C. Zhong and J.-L. Brédas, *J. Chem. Theory Comput.*, 2015, 11, 3851-3858
2. S. Yamaguchi, T. Shirasaka and K. Tamao, *Org. Lett.*, 2000, 2, 4129-4132.